THE
PHYSICAL REVIEW

A journal of experimental and theoretical physics established by E. L. Nichols in 1893

SECOND SERIES, VOL. 98, No. 3 MAY 1, 1955

Measurement of Scattering Cross Sections for Low-Energy Neutron Resonances

C. SHEER AND J. MOORE
Columbia University, New York, New York

(Received August 23, 1954; revised manuscript received December 14, 1954)

The thick-target method for the measurement of the ratio of total to scattering cross section for low-energy neutrons as a function of energy has been extended to include semi-thick targets. A family of calibration curves has been developed by means of which the measured scattered count may be interpreted in terms of (σ_s/σ_t) in the range 0–1.

The 5.19-ev and 16.6-ev levels of silver have been investigated by this method. The data agree very well with a Breit-Wigner shape over a wide range centered at the resonance, although slight deviations can be noted at distance $>\sim 10\Gamma$ away from resonance. The scattering measurements yield three independent ratios between various groups of the Breit-Wigner parameters. These ratios may be used together with transmission data to calculate the parameters. The results obtained for silver are for the 5.19-ev level: $\Gamma=0.128$ ev, $\Gamma_n=0.0155$ ev, $\sigma_{t0}=22\,200$ barns, $R_{J=1}=0.66$ barn$^{\frac{1}{2}}$; for the 16.6-ev level: $\Gamma=0.110$ ev, $\Gamma_n=0.039$ ev, $\sigma_{t0}=7300$ barns, $R_{J=0}=1.10$ barn$^{\frac{1}{2}}$; σ_p(normal element) = 5.90 barns.

I. INTRODUCTION

SLOW neutron resonances have been studied extensively in recent years. These studies[1–29] have been carried out chiefly by measurement of neutron transmission as a function of energy, and provide such quantities as the resonance energy, level spacing, and in many cases, reasonably accurate values of the level strength. In some cases, such as the Cd resonance[1,3,30] at 0.176 ev, where the capture process is predominant, and the fast neutron resonance in sulfur[31] at 108 kev, where scattering is predominant, good experimental evidence has been provided for the validity of the Breit-Wigner resonance equations. Recently, a method has been developed for measuring the ratio of scattering to total cross section as a function of energy, which is particularly applicable to resonances wherein both the capture and scattering processes are appreciable. This situation is characteristic of a large number of low-energy resonances of the medium and heavy elements. The 4.91-ev resonance in gold has been studied[32] in

[1] J. Rainwater and W. W. Havens, Jr., Phys. Rev. **70**, 136 (1946).
[2] W. W. Havens, Jr., and J. Rainwater, Phys. Rev. **70**, 154 (1946).
[3] Rainwater, Havens, Wu, and Dunning, Phys. Rev. **71**, 65 (1947).
[4] Havens, Wu, Rainwater, and Meaker, Phys. Rev. **71**, 165 (1947).
[5] Wu, Rainwater, and Havens, Phys. Rev. **71**, 174 (1947).
[6] Rainwater, Havens, Dunning, and Wu, Phys. Rev. **73**, 733 (1948).
[7] Havens, Rainwater, Wu, and Dunning, Phys. Rev. **73**, 963 (1948).
[8] R. R. Meijer, Phys. Rev. **75**, 773 (1949).
[9] F. G. P. Seidl, Phys. Rev. **75**, 1509 (1949).
[10] C. T. Hibdon and C. O. Muehlhause, Phys. Rev. **76**, 100 (1949).
[11] H. Groendijk, thesis, Groningen, 1949 (unpublished).
[12] Hibdon, Muehlhause, Selove, and Woolf, Phys. Rev. **76**, 730 (1950).
[13] M. Hamermesh and C. O. Muehlhause, Phys. Rev. **78**, 175 (1950).
[14] Harris, Muehlhause, and Thomas, Phys. Rev. **79**, 11 (1950).
[15] C. T. Hibdon, Phys. Rev. **79**, 747 (1950).
[16] S. P. Harris, Phys. Rev. **80**, 20 (1950).
[17] Harris, Hibdon, and Muehlhause, Phys. Rev. **80**, 1014 (1950).
[18] C. Heindl and I. W. Ruderman, Phys. Rev. **83**, 660 (1951).
[19] W. W. Havens and J. Rainwater, Phys. Rev. **83**, 1123 (1951).
[20] W. Selove, Phys. Rev. **84**, 869 (1951).
[21] Bernstein, Borst, Stanford, Stephenson, and Dial, Phys. Rev. **87**, 487 (1952).
[22] A. W. Merrison and E. R. Wiblin, Proc. Roy. Soc.(London) **A215**, 278 (1952).
[23] L. B. Borst, Phys. Rev. **90**, 859 (1953).
[24] Foote, Landon, and Sailor, Phys. Rev. **92**, 657 (1953).
[25] Melkonian, Havens, and Rainwater, Phys. Rev. **92**, 702 (1953).
[26] A. W. McReynolds and E. Andersen, Phys. Rev. **93**, 195 (1954).
[27] H. H. Landon and V. Sailor, Phys. Rev. **93**, 1030 (1954).
[28] Sailor, Landon, and Foote, Phys. Rev. **93**, 1292 (1954).
[29] Seidl, Hughes, Palevsky, Levin, Kato, and Sjöstrand, Phys. Rev. **95**, 476 (1954).
[30] B. N. Brockhouse, Can. J. Phys. **31**, 432 (1953).
[31] Adair, Bockelman, and Peterson, Phys. Rev. **76**, 308 (1949).
[32] J. Tittman and C. Sheer, Phys. Rev. **83**, 746 (1951).

detail by this method. Brockhouse[30] has used a similar method to study the strong capture levels in cadmium, rhodium, indium, and several rare earth elements, all at relatively low energies. It has been shown by these investigations that this type of measurement provides an additional means of evaluating the resonance level parameters; in particular, the spin of the compound nucleus.

The method consists of counting the neutrons scattered from a thick target of the element under investigation, utilizing a slow neutron spectrometer for energy determination. Although thin targets (in the sense of near unity transmission) have the advantage that the measured scattered count may be interpreted directly in terms of scattering cross section, they have the disadvantage of low counting rate and limited energy range near a resonance over which the transmission is near unity. In addition, the data generally require resolution and Doppler corrections. On the other hand, a thick target possesses none of these difficulties. A target which is thick in the wings of a resonance will be more so in the region of the peak, while the counting rate is many-fold higher. Also resolution and Doppler effects are much less important. One difficulty that exists in the use of thick targets when the percentage of scattering is not negligible, is the interpretation of scattered counts in terms of cross section. This is not available directly for thick targets because the scattered count contains an appreciable percentage of multiply scattered neutrons. Furthermore, calculation of the relationship between scattered count and target cross section involves a prohibitive amount of laborious numerical integration. The problem has therefore been resolved[32] empiricially in the following way:

The scattered count from a thick sample of the unknown target (N_x) is measured as a function of energy, together with that from a carbon reference target (N_c), alternating the targets in successive cycles. By taking the ratio N_x/N_c, the data are made independent of incident neutron flux and variation of counter efficiency. It is then easy to show that

$$N_x/N_c=\sum_{j=1}^{\infty} f_j(\theta,a_r)(\sigma_s/\sigma_t)^j, \tag{1}$$

where σ_s and σ_t are the scattering and total cross sections respectively of the unknown target, and $f_j(\theta,a_r)$ are functions of geometry and the relative thickness, (a_r), of the unknown target. ($a_r=n\sigma_t a$, where n = number of atoms per cm^3, and a = thickness in cm.) Calling this ratio F, we see that, aside from geometrical considerations, F depends in general upon the relative thickness and the ratio σ_s/σ_t. If, however, the thickness of the target is such as to satisfy the criteria: T (= neutron transmission) $\lesssim\sim 0.1$, and $\sigma_s/\sigma_t\lesssim\sim 0.5$, over the range of measurement, the target can be considered "infinitely thick." The functional dependence upon energy of the coefficients of (σ_s/σ_t) in Eq. (1) then disappears, and we may write:

$$F=\sum_{j=1}^{\infty} g_j(\theta)(\sigma_s/\sigma_t)^j, \tag{2}$$

where $g_j(\theta)$ are functions of geometry alone and are independent of the properties of the scattering nuclei. F then becomes a function of σ_s/σ_t alone and it is possible to determine this function empirically by measuring the scattered count from a standard target, satisfying the thickness criteria, for which the ratio σ_s/σ_t as a function of energy is already known. The resulting curve (Fig. 6, reference 32) may then be used to determine σ_s/σ_t from the scattered count data taken with any infinitely thick target.

Many resonances exist, however, for which the aforementioned technique would not be valid, owing to the impossibility of satisfying the criteria for infinite thickness over the range of measurement. The present paper is concerned with an extension of the method to include moderately thick targets, thus widening the scope of this type of measurement. Of particular value is the extension of the range of valid measurement further into the wings of the resonances, especially in the case of weak levels. In addition, procedures for analyzing the measured data to determine level parameters are also presented. These will be exemplified by the two lowest levels of silver, at 5.19 ev and 16.60 ev, respectively.

II. EXTENSION OF THE METHOD

From Eq. (1), the counting-rate ratio can be seen to be a function of both the relative thickness and of σ_s/σ_t whenever the target does not satisfy the criteria for infinite thickness. It follows, therefore, that the calibration in terms of a standard target for noninfinitely thick targets is valid only when the relative thickness is the same for both. When this condition prevails, the comparison is valid for any value of σ_s/σ_t. However, because of the energy dependence of a_r, which in general will not be the same for the unknown as for the standard, the comparison would be valid at only one value of the energy. This suggests the use of a family of calibration curves, each valid for a different value of a_r. Such a family of curves could be developed from measurements taken on a series of standard targets of varying thicknesses covering a sufficiently wide range of a_r and a range of σ_s/σ_t from 0 to 1. Actually, only a range of σ_s/σ_t between 0.5 and 1 need be considered since for $\sigma_s/\sigma_t<0.5$, it is always possible to satisfy the criterion $T\ll 1$ for targets of reasonable physical dimensions and therefore use the calibration curve obtained previously.

This procedure for extending the method to targets of any thickness and $\sigma_s/\sigma_t>0.5$ has one difficulty. Its use presumes a prior knowledge of a_r and therefore of σ_t as a function of energy. For most of the known resonances, this is not a serious objection since it is possible to determine with reasonable accuracy the values of σ_t

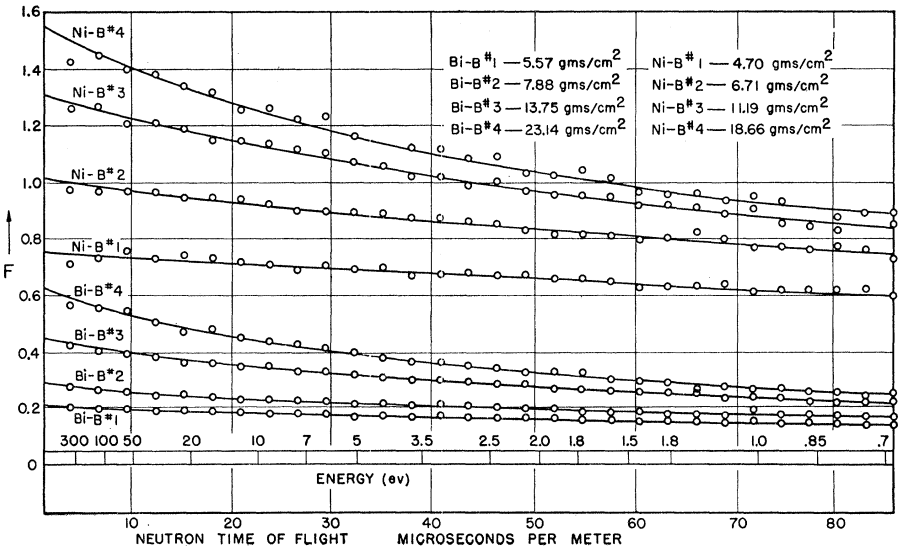

FIG. 1. Experimental curves of scattered count ratios *vs* energy used to construct the family of calibration curves for semi-thick targets ($\sigma_s/\sigma_t > 0.5$; see Fig. 3). The standard targets consist of four thicknesses each of nickel-boron and bismuth-boron mixtures.

in the wings of the resonance from transmission measurements. For the region in the vicinity of resonance where resolution effects are considerable and σ_t cannot be determined, the target usually satisfies the thick-target criteria for which the knowledge of a_r is not needed.

A series of eight standard targets were used to determine the calibration curves. Four of these consisted of a mixture of nickel and boron and the remaining four of bismuth and boron. These materials were chosen because their cross sections are slowly varying functions of energy in the range of interest (1–100 ev). The targets were fabricated by thorough mixing of the finely divided powders (<400 mesh), the Ni-B mixture consisting of 99.688 percent Ni and 0.312 percent B,[33] whereas the Bi-B mixture consisted of 99.540 percent Bi and 0.460 percent B. The thickness for each set varied from ~5 to 20 g/cm². The proportions were calculated to give a range of variation for σ_s/σ_t from 0.45 to 0.99. The thickness range was chosen so as to cover values of relative thickness from about 0.2 to 4.0. The lower limit was dictated by counting-rate considerations and the upper limit by the fact that for $a_r > \sim 4$, the target satisfies the criteria for a thick target. The mixtures were canned in welded aluminum containers of the appropriate shape.

The apparatus used has already been adequately described.[32] The scattering measurements for these targets were taken in the usual manner, except that the B^{10} background target was used as a backing for each target measured. This was done because the targets involved were no longer infinitely thick and it became necessary to prevent background neutrons which were scattered from the walls of the chamber from passing through the target to the counters. Such neutrons would result in an erroneous background count. This technique was subsequently used for all semi-thick targets. The total count from each target was high enough to assure virtually negligible statistical error (<1.0 percent) at each energy. Residual errors were due to random fluctuations in the detection and measuring equipment. The results of this measurement are shown in Fig. 1 wherein the ratio of scattered counts of each standard target to that of the carbon reference target (F) is plotted *vs* energy.

The values of a_r and σ_s/σ_t for the standard targets were determined experimentally from transmission data, shown in Fig. 2. The total cross section for these mixtures can be evaluated directly from the transmission measurements, since they are linear functions of energy in this region ($1/v$) and resolution effects do not enter. The straight lines represent least square fits to the experimental points. The percentages of scattering and hence, the values of σ_s/σ_t at each energy, are determined from the slopes and intercepts of these lines.

The final calibration curves are obtained from the experimental data in the following manner. For a particular value of σ_s/σ_t, the time of flight at which one of the standard samples has this value of σ_s/σ_t is determined. The four values of F for the four thicknesses of the appropriate samples are obtained for this time of flight from the data in Fig. 1. The values of a_r for the four samples are obtained from the data in Fig. 2 and the known thickness of the sample. This procedure is repeated for the second sample and the function F is then plotted against a_r for the particular value of σ_s/σ_t

[33] The boron was in the form of microcrystalline powder prepared by the Cooper Metallurgical Associates, Cleveland, Ohio.

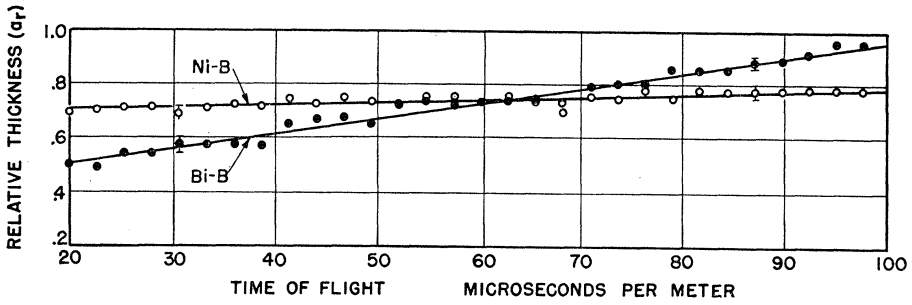

FIG. 2. Curves of relative thickness *vs* time of flight obtained from transmission of the nickel-boron and bismuth-boron mixtures used for the standard targets. Target thicknesses: Ni-B—3.701 g/cm²; Bi-B—13.98 g/cm².

selected. The resultant curves, for values of σ_s/σ_t ranging from 0.50 to 1.0 in steps of 0.05, are shown in Fig. 3. This is the family of calibration curves used in these experiments for semi-thick targets.

It should be noted that, of the eleven curves exhibited, only the upper four have eight experimental points, corresponding to the four thicknesses of each standard sample. The rest have only four, except for the lowest ($\sigma_s/\sigma_t=0.50$) for which a point located on the extreme right was obtained from the calibration curve for infinitely thick targets which is valid for $\sigma_s/\sigma_t=0.50$. The value of F for this point may be associated with any value of a_r down to a value where $\exp(-a_r)\sim 0.1$. In order to obtain experimental points to complete the set of curves in the region of higher a_r for σ_s/σ_t between 0.55 and 0.80 it would have been necessary to run additional standard targets. For the sake of economy in cyclotron time, the remainder of the points were obtained by extrapolation from existing data. The method of extrapolation is shown in Fig. 4 where values of F *vs* σ_s/σ_t are plotted for fixed values of a_r. These curves were obtained from Fig. 3 in regions where experimental points determine the shape of the curves. The curves of σ_s/σ_t *vs* F in Fig. 4 are nearly linear on a semilog plot below about $\sigma_s/\sigma_t=0.80$, so that selection of points between 0.50 and 0.80 to fill in the calibration curves is simple. Only points from this linear region were required to complete the set in Fig. 3.

The validity of the new set of calibration curves was checked by using some of the experimental points in the curve of σ_s/σ_t *vs* energy for the 4.91-ev gold resonance previously reported. This curve is shown in Fig. 5 where in the solid line represents the theoretical Breit-Wigner curve for the level, using parameters determined

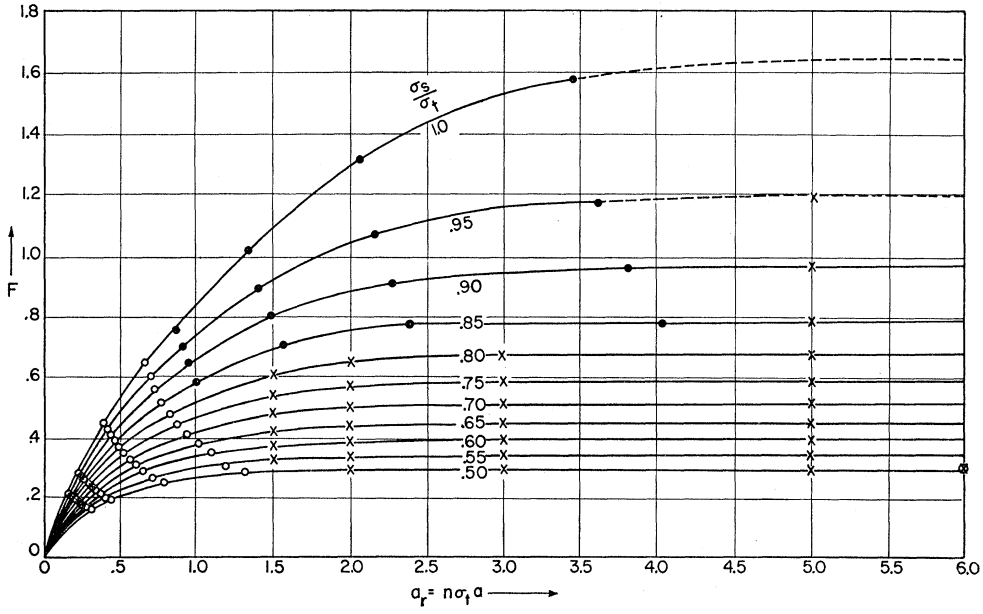

FIG. 3. Calibration curves for neutron scattering from semi-thick targets ($0.5<\sigma_s/\sigma_t<1.0$). The points used to construct these curves were taken from the following sources: ● nickel-boron standard targets; o bismuth-boron standard targets; × extrapolated points from curves of Fig. 4; ⊗ calibration curve for infinitely thick targets (Fig. 6, reference 32).

by fitting the experimental data (open circles). As may be seen, a good fit to the dispersion formula is obtained in the range for which $\sigma_s/\sigma_t<0.5$. However, on the left are five points for which $\sigma_s/\sigma_t>0.5$, for which the calibration curve for infinitely thick targets is not valid, and for which it was consequently predicted that they would fall below the theoretical curve, as shown in the figure. The calibration curves of Fig. 3 were then used to determine σ_s/σ_t from the original data for these points. The resulting values of σ_s/σ_t (black dots) now fall on the theoretical curve, which, since this is an isolated level, tends to confirm the validity of the new calibration curves. It is significant that four of these five points required the use of the new curves in the region where it was filled in by extrapolation.

The shape of the curves in Fig. 3 indicates that, for $a_r>\sim2.0$ and $\sigma_s/\sigma_t<\sim0.9$, the conversion of F to σ_s/σ_t is insensitive to the value of a_r. Consequently, for most applications only a very rough knowledge of σ_t is required in advance. In the region where the curves slope more rapidly (high σ_s/σ_t and low a_r), for which more accurate values of a_r are needed, the curves are generally used only for the wings of the resonance where such values of σ_t are available from transmission measurements. In the rare cases where this is not so (weak resonances having high Γ_n/Γ), a trial and error procedure may be used. Using transmission data as a guide, one may guess values of σ_t in this region as a first approximation to be successively refined by curve-fitting.

III. DOPPLER EFFECT

Since the ratio σ_s/σ_t is the quantity measured in these experiments and since Doppler effect should broaden the resonant peaks of σ_s and σ_t in the same manner, the effect on their ratio is expected to be small. This was tested by applying Doppler correction[34] to the Breit-Wigner equations for capture and scattering, including in the latter Doppler broadening of the interference term. The approximations involved in this computation are the assumption of a Maxwellian gas model for the target and the neglect of the factor $(E_0/E)^{\frac{1}{2}}$ in the capture cross section, which is very nearly unity in the range investigated. Neither approximation leads to appreciable error.

Since this effect would be most noticeable in cases like the Ag 16.6-ev level, where the ratio of natural to Doppler width appears to be relatively low, the parameters of this level as determined below were used to make a computation of σ_s/σ_t, with and without Doppler correction. The results are shown in Fig. 6. The solid line represents the theoretical Breit-Wigner curve of σ_s/σ_t without Doppler correction. The effect of the correction is indicated by the dashed line. The deviation of the latter from the uncorrected curve is small, and extends over a very limited region near resonance. It arises mainly from the fact that the Doppler effect

[34] H. Bethe, Revs. Modern Phys. **9**, 140 (1937).

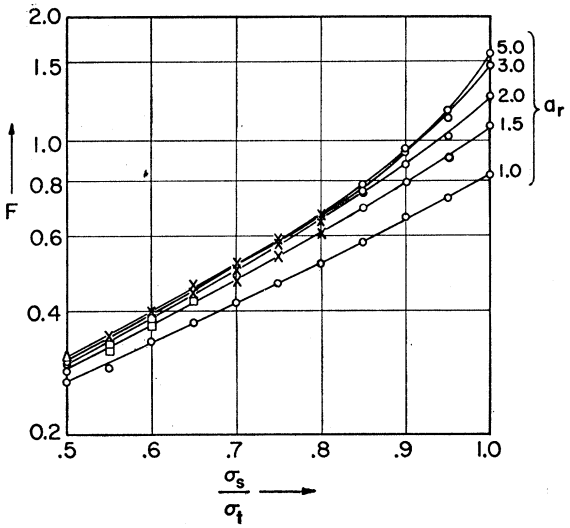

FIG. 4. Semilog plot of F *vs* σ_s/σ_t used to obtain points to complete the calibration curves of Fig. 3. These points (crosses) were interpolated on the above curves which were first drawn on the remaining points. The latter were obtained from the following sources: O points from scattering data of Fig. 1; □ points from slight extrapolation of curves of Fig. 1; △ point from calibration curve for infinitely thick targets.

flattens the region of the peaks very close to resonance, so that in this region σ_s/σ_t would remain more constant than it would for the sharp resonance peaks of the natural level. The deviation is too small to affect the

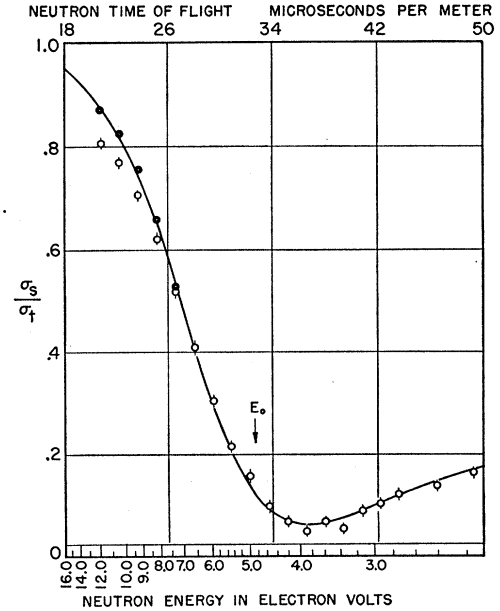

FIG. 5. Portion of curve of σ_s/σ_t *vs* energy for the gold 4.91-ev resonance[32] measured previously. The open circles represent the experimental points using the calibration curve for infinitely thick targets, valid for $0<\sigma_s/\sigma_t<0.5$. The black circles represent the same data using the calibration curves of Fig. 3. The solid curve is a theoretical Breit-Wigner curve with parameters adjusted for the best fit.

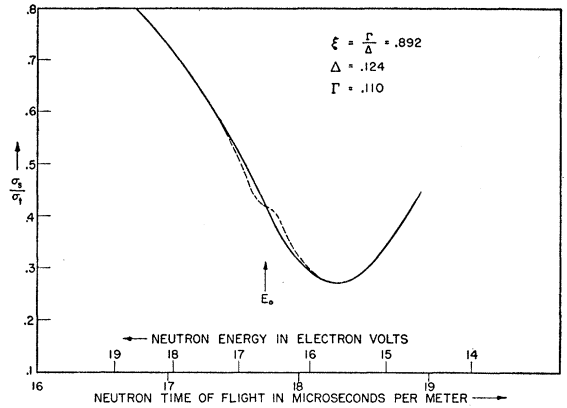

FIG. 6. Doppler effect on σ_s/σ_t in vicinity of the silver 16.6-ev resonance. Dashed curve is corrected, whereas solid line is uncorrected, for Doppler effect.

evaluation of resonance parameters from the data and would in any case be hidden by the effects of instrument resolution. As far as the present measurements are concerned, therefore, it is significant only insofar as it affects the recoil energy-loss correction,[35,36] in a small region near resonance, where this correction is determined by a Doppler broadened curve of total cross section. The net effect is therefore to reduce the magnitude of the correction.

IV. SCATTERING MEASUREMENTS ON SILVER

The experimental procedures followed in the scattering measurements on the two lowest resonances of silver were essentially the same as that established for the gold measurements.[32] The only difference is the use of a B^{10} target as a backing for the silver and carbon targets in addition to its use as a background target. This was done to avoid erroneous background measurements, since part of the curves for both resonances extended to the semithick region. The silver target was a slab 4 in.×6 in. and $1\frac{1}{2}$ in. thick, having the smaller surfaces bevelled at 45° so as to present an area of 4 in.×4 in. to the beam with uniform slant thickness of 2.12 in. The effective target thickness in the direction of the beam was 57 g/cm².

[35] This correction was originally calculated (see reference 32) for the gold scattering data on the assumption of a stationary free-atom model for the target. Brockhouse and Hurst (see reference 36) have worked out the correction more carefully taking into account thermal motion of the target atoms, both bound and free. Because of the neglect of this motion, Brockhouse (see reference 30) estimated that some of the parameters reported by Tittman and Sheer for the gold resonance would be in error by about 10 percent. Accordingly, the present authors calculated the energy loss correction for this case (as well as the silver 5.19-ev level) using the improved method, and found the difference to be negligible. The reasons for this are that the correction is reduced by instrument resolution in addition to Doppler broadening, and that it is significant for such a small region relative to the range of measurement that the experimental points involved can be omitted without materially affecting the results of the curve-fitting process.

[36] B. N. Brockhouse and D. G. Hurst, Phys. Rev. 88, 542 (1952).

The 5.19-ev resonance was measured with instrument resolution widths of 6.15, 3.8, 3.1, and 2.4 microseconds per meter, full width at the base of the resolution triangle. No change in the curve was noted for resolution widths of 3.8 microseconds per meter or less, indicating that the curve is completely resolved under these conditions. The 16.6-ev resonance was studied with a 2.4 microseconds per meter resolution. The curve for this level is not quite resolved. Resonances below about 10 ev are completely resolved with resolution widths of 2.4 microseconds per meter and nearly so up to about 30 ev. Since this width represents the lowest that can be used with the present apparatus, consistent with reasonable running time, it was not feasible to resolve this level.

V. ANALYSIS OF THE DATA

The experimental curves of σ_s/σ_t *vs* energy in the region of a resonance provide information which, when used in conjunction with transmission data, permits the evaluation of all of the resonance constants. All of these except J may, in principle at least, be evaluated by a curve-fitting process from the transmission data (σ_t *vs* energy) alone. The advantage of using thick target scattering data in curve-fitting is that, for the same percentage error in the measurements, a curve of σ_s/σ_t *vs* E is inherently capable of providing more accurate values for some of the parameters than a curve of σ_t *vs* E.

The Breit-Wigner one-level dispersion formulas form the basis for the analysis. These will be used in the following form:

$$\sigma_c=\frac{\sigma_{c0}\Gamma^2(E_0/E)^{\frac{1}{2}}}{4(E-E_0)^2+\Gamma^2}, \tag{4}$$

$$\sigma_s=\sigma_p+\frac{X+Y(E-E_0)}{4(E-E_0)^2+\Gamma^2}, \tag{5}$$

where E_0=energy of exact resonance, σ_{c0}=capture cross section at resonance, $\Gamma=\Gamma_n+\Gamma_\gamma$=total level width, Γ_n=neutron width, Γ_γ=width for radiative capture, $X=4\pi G_J\lambda_0^2\Gamma_n^2$, $Y=16\pi G_J\lambda_0\Gamma_nR$, $\sigma_p=4\pi G_JR^2+4\pi G_J'R'^2$, =total potential scattering cross section, G_J, G_J'=spin weight factors for the resonant and non-resonant spin states of the compound nucleus, respecgively, R, R'=effective nuclear radii for the resonant and non-resonant spin states.

Equations (4) and (5) are for monoisotopic targets. When more than one isotope is present, the cross section for an element containing k isotopes is given by

$$n\sigma=n_1\sigma_1+n_2\sigma_2+\cdots+n_k\sigma_k,$$

where $\sigma_1\cdots\sigma_k$=cross sections for the individual isotopes, $n_1\cdots n_k$=number of atoms of each isotope per cm² of target, n=number of atoms of all kinds per cm² of target, σ=cross section of the natural element. Thus,

we may write

$$\sigma=\sum_{i=1}^{k} G_{Ii}\sigma_i,$$

where $G_{Ii}=n_i/n=$isotopic fraction.

In the case of silver, there are two isotopes of nearly equal abundance: Ag^{107}, for which $G_I=0.5135$, and Ag^{109}, for which $G_I=0.4865$. Furthermore, the 5.19-ev resonance is known[11] to occur in Ag^{109} whereas the 16.6-ev resonance occurs in Ag^{107}. In all of the subsequent discussion, the subscript "1" will be used to refer to Ag^{109} and hence to the 5.19-ev resonance, while the subscript "2" will refer to Ag^{107} and the 16.6-ev resonance. Since the two resonances occur in different isotopes, there is no possibility of interference between the levels, and the cross sections for natural silver will be given by

$$\sigma_c=\frac{G_{I1}(\sigma_{c0}\Gamma^2)_1(E_{01}/E)^{\frac{1}{2}}}{4(E-E_{01})^2+\Gamma_1^2}+\frac{G_{I2}(\sigma_{c0}\Gamma^2)_2(E_{02}/E)^{\frac{1}{2}}}{4(E-E_{02})^2+\Gamma_2^2}, \quad (6)$$

$$\sigma_s=\sigma_p+\frac{X_1+Y_1(E-E_{01})}{4(E-E_{01})^2+\Gamma_1^2}+\frac{X_2+Y_2(E-E_{02})}{4(E-E_{02})^2+\Gamma_2^2}. \quad (7)$$

The potential scattering for natural silver consists of four components, two each for the resonant and nonresonant spin states for each isotope. The factors G_{I1} and G_{I2} in Eq. (6) will be omitted in the subsequent discussion, and the quantities $(\sigma_{c0}\Gamma^2)_1/(\sigma_{c0}\Gamma^2)_2$ will be assumed to be multiplied by the approximate isotope factor. The subscripts will also be omitted in other cases where there is no chance of ambiguity.

The quantities involving the level parameters which may be obtained directly from the measured curve of σ_s/σ_t, when the resonance is completely resolved, are the following ratios: Γ_n/Γ, $\sigma_{c0}\Gamma^2/\sigma_p$, and Y/σ_p. The ratio X/σ_p is easily shown to be obtainable from the first two of these. The evaluation of all of the Breit-Wigner parameters of the level from these quantities requires the independent knowledge of three additional data. A convenient choice for these three quantities consists of the resonance energy, E_0, the spin weight factor, G_J, and any one of the quantities $\sigma_{t0}\Gamma^2$, σ_p, X, or Y. For most of the strong, low energy resonances, this auxiliary information may be obtained from transmission measurements, particularly those taken on recently developed high resolution neutron spectrometers. In particular, the resonance energy has been measured for a large number of resonances with high precision. Also values of the level strength $(\sigma_{t0}\Gamma^2)$ for a number of resonances, as determined by independent investigators have shown a high degree of consistency. Finally, the spin weight factor, G_J, can be determined with the aid of high resolution measurements of the peak total cross section. The scattering data yield the quantity Γ_n/Γ directly. This is equal to the value of σ_s/σ_t at resonance. Thus, using the relation $\sigma_{t0}=4\pi G_J\lambda\!\!\!^{-}_0{}^2$ $\times(\Gamma_n/\Gamma)$ one may calculate two alternative values of σ_{t0} corresponding to the two possible values of G_J. Comparison of the values so calculated with those obtained by transmission measurements often enables a unique choice of G_J to be made, which is consistent with both the scattering and transmission data. In particular, if the experimental value of σ_{t0} lies definitely between the two calculated values, the smaller value is at once ruled out since measured values of σ_{t0} are always less than the true value owing to resolution and Doppler effects. This method of determining G_J is especially good where the resonance occurs in an isotope of small nuclear spin for which the alternative values of σ_{t0} are far apart.

When E_0, G_J, and $\sigma_{t0}\Gamma^2$ are known, the remainder of the level parameters may be determined by analysis of the measured curve of σ_s/σ_t *vs* energy as described in the previous paper on gold. However, the curve-fitting process may be simplified by replacing σ_s/σ_t with σ_s/σ_c via the relation $\sigma_s/\sigma_c=(\sigma_s/\sigma_t)/(1-\sigma_s/\sigma_t)$. If we divide Eq. (5) by Eq. (4) and multiply through by $(E_0/E)^{\frac{1}{2}}$, we obtain:

$$(\sigma_s/\sigma_c)(E_0/E)^{\frac{1}{2}}=(4\sigma_p/\sigma_{c0}\Gamma^2)(E-E_0)^2+(Y/\sigma_{c0}\Gamma^2)(E-E_0)+(X+\sigma_p\Gamma^2)/\sigma_{c0}\Gamma^2. \quad (8)$$

Equation (8) represents a parabola in the form $y=ax^2+bx+c$, where $y=(\sigma_s/\sigma_c)(E_0/E)^{\frac{1}{2}}$, $x=E-E_0$, $a=4\sigma_p/\sigma_{c0}\Gamma^2$, $b=Y/\sigma_{c0}\Gamma^2$, and $c=(X+\sigma_p\Gamma^2)/\sigma_{c0}\Gamma^2=X/\sigma_{c0}\Gamma^2+\sigma_p/\sigma_{c0}$. Since generally $\sigma_p\ll\sigma_{c0}$, we may write for the constant term of the parabola: $c=X/\sigma_{c0}\Gamma^2$. Thus, after the experimental values of σ_s/σ_t have been converted into $(\sigma_s/\sigma_c)(E_0/E)^{\frac{1}{2}}$, a quadratic least-squares fit to these on an $E-E_0$ scale is performed. This yields the numerical values of a, b, and c for the parabola which best fits the data in the range of measurement.

Having determined the constants a, b, and c, the Breit-Wigner parameters may then be calculated from the value of the level strength with the aid of Eqs. (4) and (5) and the following relations:

$$\Gamma_n/\Gamma=c/(c+1);\quad \sigma_{c0}\Gamma^2=\sigma_{t0}\Gamma^2(1-\Gamma_n/\Gamma);$$
$$X=c(\sigma_{c0}\Gamma^2);\quad Y=b(\sigma_{c0}\Gamma^2);\quad \sigma_p=\tfrac{1}{4}a(\sigma_{c0}\Gamma^2). \quad (9)$$

5.19-ev Resonance of Silver

The above analysis was carried out on the scattering data for the 5.19-ev level of silver on the assumption that this is an isolated resonance in the range of measurement (0.7 to 9.0 ev). The result of the least squares fit is shown by the dashed line parabola of Fig. 7. Inspection shows that although the experimental points appear to fit this curve well in the wings, they are consistently below the curve in the region of the minimum, close to resonance. Since this effect could be caused by the contribution of higher energy resonances, and possibly a level of negative energy near zero, the procedure was repeated using a more restricted range close to resonance; (below the horizontal dashed line in Fig. 7). The results are shown by the solid-line

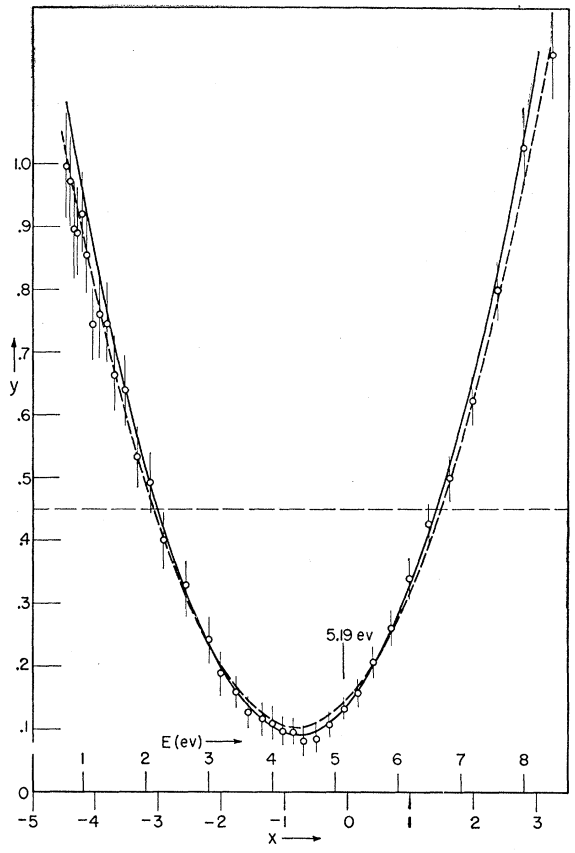

FIG. 7. Parabolic curves of $(\sigma_s/\sigma_c)(E_0/E)^{\frac{1}{2}}$ as a function of $E-E_0$ for the silver 5.19-ev level. The solid curve represents a least-squares fit to the data below the horizontal dashed line, while the dashed curve is the fit to all the data.

parabola of Fig. 7. This curve appears to fit the data well near the minimum but not in the wings. Since the distorting effects of other levels (see discussion below) should be negligible near resonance, the constants of this parabola were used to calculate the level parameters

TABLE I. Table of parameters for the 5.19-ev and 16.6-ev resonances of silver. Quantities marked with an asterisk represent auxiliary data from other measurements. Values are for the normal element except where noted.

E_0	*5.193 ev	*16.60
$\sigma_{t0}\Gamma^2$	*366 b-ev^2	90 b-ev^2
J	1	0
Γ_n/Γ	0.121±0.007	0.35±0.05
Γ	0.128±0.016 ev	0.11±0.013 ev
Γ_n	0.0155±0.0022 ev	0.039±0.006 ev
σ_p	5.90±0.37 b	5.90±0.37 b
X	44.43±3.17 b-ev^2	31.5±4.1 b-ev^2
Y	37.80±2.59 b-ev^2	31.6±3.8 b-ev^2
R	0.66±10 barn$^{\frac{1}{2}}$	1.10±0.11 barn$^{\frac{1}{2}}$
σ_{t0}	22 200 b	7300 b
σ_p (isotope)	*4.64 b	7.09 b
R'	0.42 barn$^{\frac{1}{2}}$	0.65 barn$^{\frac{1}{2}}$

in accordance with the relations (9). These are:

$$a=0.0734\pm0.0040;\quad b=0.1175\pm0.0071;$$
$$c=0.1381\pm0.0088.$$

Values of 366±10 b-ev^2 for $\sigma_{t0}\Gamma^2$ and 5.193±0.005 ev for E_0 were used for the computation of the level parameters. These represent the results of the most recent measurements[37] at Brookhaven and agree remarkably well with independent measurements of other investigators.[20,28,29] The choice of a value for J was relatively easy in this case since, of the two alternative values of σ_{t0} calculated with the aid of the first of Eqs. (9), the one corresponding to $J=0$ was considerably lower than the peak cross section as measured directly in transmission experiments. The choice of $J=0$ is therefore ruled out, and J was taken to be 1.

A list of parameters calculated on the above basis is shown in the first column of Table I. The calculation of R', the effective radius for the nonresonant spin-state, required the knowledge of an additional independent datum. This arises from the existence of two isotopes in silver, only one of which is responsible for the resonance. Although in the above analysis, the second term on the right of Eq. (6) and the third on the right of Eq. (7) were assumed negligible, the constant term in Eq. (7) σ_p, now contains an additional component. It should be written

$$\sigma_p=4\pi g_1R_1^2+4\pi g'R_1'^2+G_{I2}\sigma_{p2}, \qquad (10)$$

where σ_{p2} is the contribution of the nonresonant isotope (Ag^{107}) to the potential scattering of the element. Since the scattering measurement fixes only R_1, in addition to σ_p, the potential scattering of either Ag^{107} or Ag^{109} must be known. If σ_{p2} is known, R_1' may be determined from Eq. (10). If σ_{p1} is known, R_1' may be determined from the relation: $G_{I1}\sigma_{p1}=4\pi g_1R_1^2+4\pi g_1'R_1'^2$.

The assumption may be made that the contributions to the total potential scattering of the two spin-states of Ag^{110} are in the proportion of their respective spin weight factors. This is equivalent to assuming equal nuclear radii for the two spin-states ($R_1=R_1'$). From this assumption we obtain $\sigma_{p1}=5.47$ b and $\sigma_{p2}=6.31$ b. The assumption that the nuclear radii for the two spin-states are equal, is, however, open to question, since the corresponding quantities were found to differ in the case of the 4.9-ev level[32] in gold, and in sodium and cobalt[38] as well. An independent measurement of the isotopic potential scattering would be preferable. Such a measurement has been made by Hibdon and Muehlhause[39] who determined both σ_{p1} and σ_{p2} by counting neutrons scattered from thin foils of normal and enriched silver, using cadmium and thick silver filters to remove both thermal and resonance neutrons from the beam. They obtained the values $\sigma_{p1}=4.64$ b; $\sigma_{p2}=7.91$ b. Using the value of σ_{p1} as the independent

[37] R. E. Wood (to be published).
[38] C. O. Muehlhause, Phys. Rev. **79**, 1002 (1950).
[39] C. O. Muehlhause (private communication).

datum yields $R_1'=0.42$ b. The same value of σ_{p1} may be used together with the value of σ_p obtained from the present measurements to calculate σ_{p2} by Eq. (10) as a check on over-all consistency. When this is done, a value of $\sigma_{p2}=7.09$ b. is obtained which is $\sim$10 percent lower than the measured value of 7.91 b. On the other hand, using $\sigma_{p2}=7.91$ as the independent datum yields $\sigma_{p1}=3.78$ b which is slightly less than $4\pi g_1 R_1^2$ as determined from the scattering data. This would require R' to be essentially zero within the accuracy of the measurements. These results are summarized in Table II.

A curve of σ_s/σ_t *vs* energy based on the parameters given in the first column of Table I is shown in Fig. 8. The range of analysis is indicated by the vertical dashed lines marked A and B. The slight deviations of the data from a true Breit-Wigner single-level shape can be noted in the high- and low-energy regions, although it is not as apparent here as when plotted in the parabolic form of Fig. 7.

16.6-ev Resonance of Silver

The analysis of the 16.6-ev resonance was complicated by two factors: (1) The strong level at 5.19 ev contributes appreciably to the experimental curve near the 16.6-ev level. (2) The experimental curve for this level is not completely resolved. The former difficulty requires the use of all terms in Eqs. (6) and (7), and merely increases the computational labor since the parameters for the 5.19-ev level are available. The latter precludes the parabola method of analysis discussed above. A trial and error procedure was therefore adopted for this level.

TABLE II. Values of isotopic potential scattering and nonresonant spin state nuclear radius computed from several assumed independent data together with the value of σ_p (potential scattering of the element=5.90 b) derived from the present experiment.

Assumed as the independent datum	Computed from assumed datum
$R_1=R_1'$	$\sigma_{p1}=5.47$ b; $\sigma_{p2}=6.31$ b; $R_1'=0.66$ barn$^{\frac{1}{2}}$
$\sigma_{p1}=4.64$ b	$\sigma_{p2}=7.09$ b; $R_1'=0.42$ barn$^{\frac{1}{2}}$
$\sigma_{p2}=7.91$ b	$\sigma_{p1}=3.78$ b; $R_1'\cong 0$

In the first trial analysis a value of 23 for $\sigma_{t0}\Gamma^2$ was used, which was obtained from the transmission measurements[40] of Merrison and Wiblin.[22] This appeared to agree with an early rough value of 25 obtained at Columbia.[3] The procedure used was as follows: Using $\sigma_{t0}\Gamma^2=23$, a value of Γ_n/Γ was assumed which gives $\sigma_{c0}\Gamma^2$, Γ, and Γ_n. Using for R_2 the values $\sigma_{p2}/4\pi$, the constants X_2 and Y_2 were calculated and a curve of σ_s/σ_t *vs* energy computed from Eqs. (6) and (7). This curve, however, could not be compared directly to the experimental curve since the latter is not completely resolved. Therefore, the calculated curve is translated into a curve of scattered counts (F) *vs* energy by means of the calibration curves. This resulted in the curve that would have been measured with perfect resolution if the assumed parameters had been correct. In order to make a comparison to the measured data, a resolution function

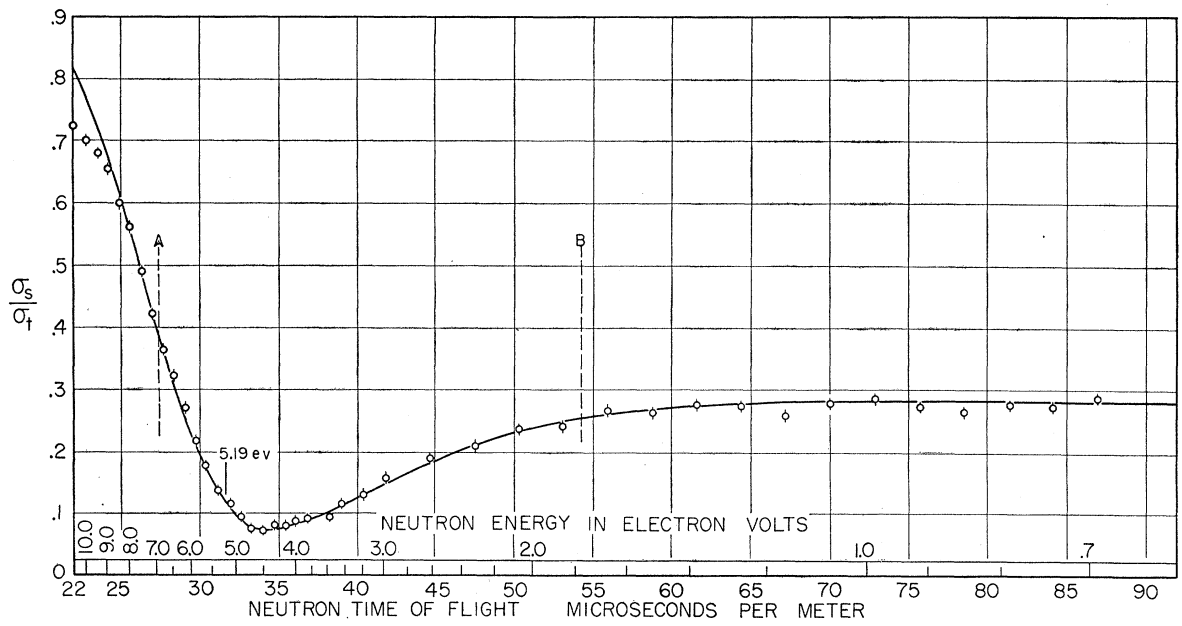

FIG. 8. Curve of σ_s/σ_t *vs* energy for the 5.19-ev level of silver. Solid line represents theoretical Breit-Wigner curve using parameters obtained by a least-squares fit of the data in the range AB.

[40] After the analysis of this level was completed, the paper by Seidl *et al.* (see reference 29) was published reporting a value of 31 b-ev^2. This value would not alter significantly the results of the ensuing analysis.

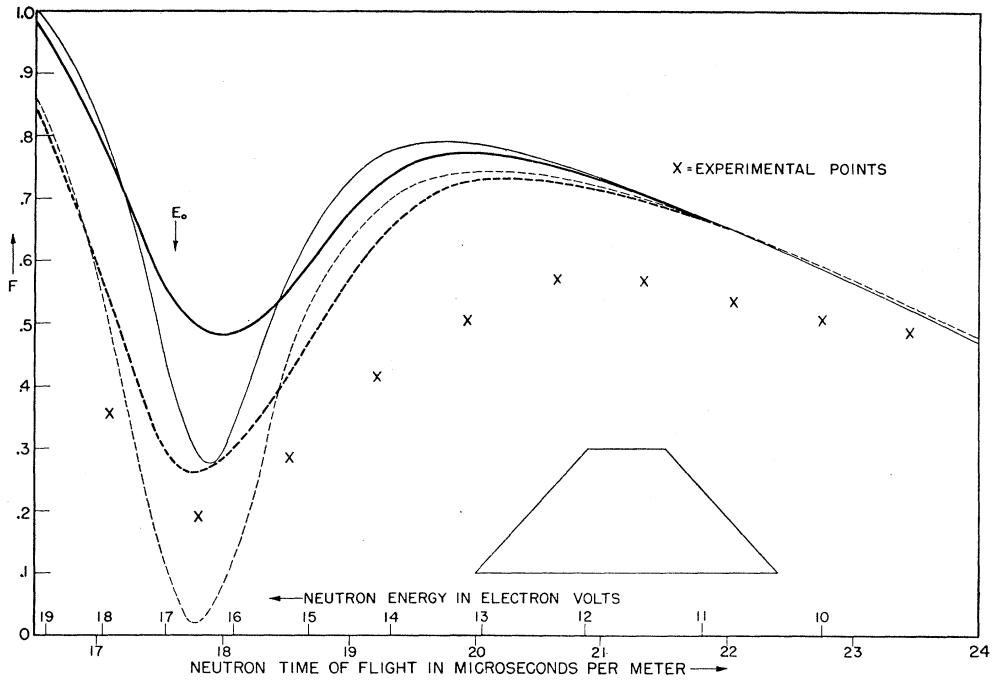

FIG. 9. Calculated scattering curves for the 16.6-ev level of silver on the basis of $\sigma_{t0}\Gamma^2=23$. The solid line and dashed curves were calculated with $\Gamma_n/\Gamma=0.5$ and 0.05 respectively. The thin lines represent the theoretical curves, and the heavy lines are the result of applying the resolution function shown, and which should be compared to the experimental points (crosses).

appropriate to the apparatus must be applied to the calculated F *vs* energy curve. Since the resolution function is known only approximately, the results of fitting such a curve to experimental data are necessarily less accurate than if the experimental curve were completely resolved. Fortunately, the present case is one in which the data are only slightly altered by resolution effects, so that the uncertainties in the shape and width of the resolution function are not too important.

A series of such curves were computed for values of Γ_n/Γ ranging from 0.05 and 0.5. Two of these, corrected for resolution, are shown in Fig. 9 for the choices of Γ_n/Γ, 0.05 and 0.5. The crosses represent the experimental points without the correction for recoil energy loss. However, this correction will materially affect only points near resonance. Points lying above about 19 microseconds per meter will be practically unaffected. Nevertheless, Fig. 9 indicates marked disagreement between the experimental data and the curves calculated on the basis of $\sigma_{t0}\Gamma^2=23$ for a wide range of Γ_n/Γ throughout the range of measurement. Furthermore, the disagreement could not be eliminated by varying either the resolution function or the value of R_2. It was tentatively concluded, therefore, that the available values of $\sigma_{t0}\Gamma^2$ were inconsistent with the present data.

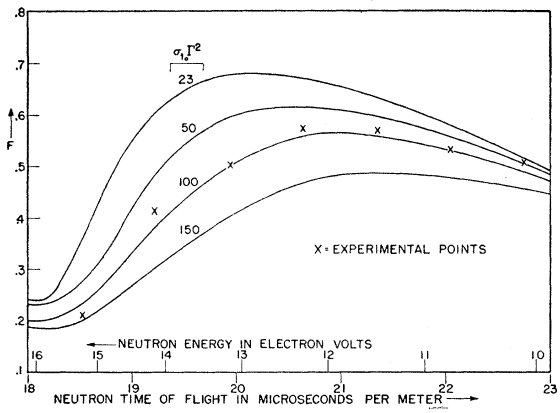

FIG. 10. Scattering curves for the 16.6-ev level of silver calculated on the basis of $\Gamma_n/\Gamma=0.40$ for four values of $\sigma_{t0}\Gamma^2$.

A wide range of both $\sigma_{t0}\Gamma^2$ and Γ_n/Γ were then investigated and plotted in various combinations. In each case, the resolution function was applied to the calculated curve and the results compared to the data. It was found impossible to match the shape of the experimental curve unless a value of $\Gamma_n/\Gamma\sim0.4$ was used. Figure 10 shows a set of four calculated curves for which $\Gamma_n/\Gamma=0.4$ and $\sigma_{t0}\Gamma^2=23$, 50, 100, and 150 respectively. It is interesting to note that when Γ_n/Γ is close to 0.5 the curve of σ_s/σ_t *vs* energy is sensitive to the quantity $\sigma_{c0}\Gamma^2$ in the wings of a resonance. Figure 10 shows this effect to be strongest for the 16.6-ev resonance in the region between 18 and 23 microseconds per meter, where resolution effects and the energy loss corrections are unimportant. Consequently, the match in this region was used as the basis for the tentative

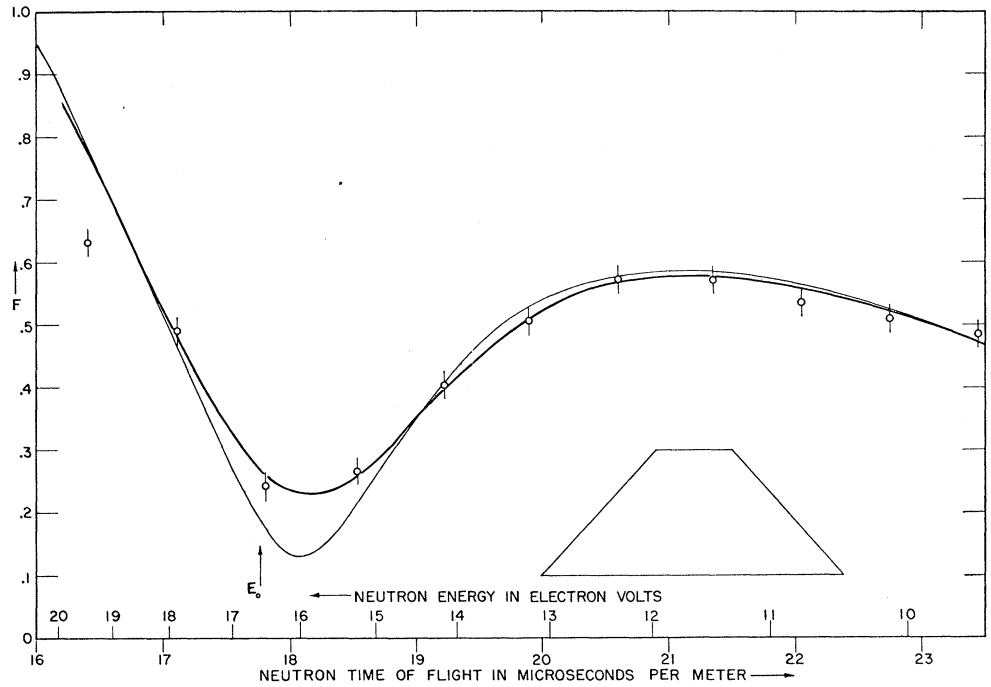

FIG. 11. Scattering curve for the 16.6-ev level of silver representing the best fit to the experimental data. Parameters used were $\sigma_{t0}\Gamma^2=90$ b-ev^2, $\Gamma_n/\Gamma=0.35$, $\sigma_p=5.90$ b. The thin line represents the calculated curve while the heavy line is the result of applying the resolution function.

choice of $\sigma_{c0}\Gamma^2$. The values $\Gamma_n/\Gamma=0.4$ and $\sigma_{t0}\Gamma^2=100$ were used to complete the first trial analysis.

With these parameters as a starting point, the fit was successively refined by trial and error. The best fit was obtained for the values $\Gamma_n/\Gamma=0.35$, $\sigma_{t0}\Gamma^2=90$ b-ev^2, $X_2=31.5$ b-ev^2, and $Y_2=31.6$ b-ev^2. A curve based on these parameters is shown in Fig. 11. All corrections have been applied to the data. The thin line represents the calculated curve and the heavy line is the result of applying the resolution function. The latter matches the experimental points fairly closely except for the point on the left, where the effect of the next level (31 ev) would be expected to become noticeable. In order to check the sensitivity of this analysis, particularly in view of the comparatively high values of Γ_n/Γ and $\sigma_{t0}\Gamma^2$ obtained, a series of curves were plotted in which these quantities were varied and the results compared to the experimental data. This is shown by the three curves of Fig. 12. They indicate that an uncertainty $\sim\pm15$ percent should be assigned to the above values of Γ_n/Γ and $\sigma_{t0}\Gamma^2$.

Since no independent measurement of σ_{t0} for this level could be found providing a value intermediate between the two possible values indicated by the present results, no definite assignment of J could be made. However, a tentative choice was made with the aid of a measurement of the resonance absorption integral. This quantity, denoted by Σ_a, has been measured by Harris *et al.*,[17] and is given by

$$\Sigma_a=(\pi/2)4\pi\lambda\!\!\!^{-}_0{}^2(G_J\Gamma/E_0)\Gamma_n/\Gamma(1-\Gamma_n/\Gamma).$$

Using the value $\Sigma_a=80.6$ b, reported by these investigators, and $\Gamma_n/\Gamma=0.35$ from the present analysis, one obtains $G_J\Gamma=0.023$. Inserting the values $\Gamma_n/\Gamma=0.35$ and $\sigma_{t0}\Gamma^2=90$ b-ev^2 into the relation

$$\sigma_{t0}\Gamma^2=4\pi\lambda\!\!\!^{-}_0{}^2g(\Gamma_n/\Gamma)\Gamma^2,$$

one obtains $G_J\Gamma^2=0.003$. From these two figures $G_J=0.18$ is obtained, which is more consistent with $\frac{1}{4}$ ($J=0$) than with $\frac{3}{4}$ ($J=1$). Accordingly, a tentative assignment of $J=0$ was made for the spin state of Ag^{108} responsible for this resonance.

The second column of Table I contains a list of the level parameters based on the above evaluation.

DISCUSSION

It appears to be characteristic of the type of cross section measurement described in this paper that it leads to values of the peak total cross section in general higher than those obtained from other measurements. When the thick-target scattering technique was first used to study the gold 4.91-ev level,[32] the resulting value for σ_{t0} (24 600 b) required by the choice $J=1$,[41,42]

[41] In view of the recent transmission measurement, the values $J=1$, originally chosen for Au^{198}, must be ruled out. The value $J=2$, as reported by Wood (reference 42), appears to be the correct choice.

[42] R. E. Wood, Phys. Rev. **95**, 644(A) (1954).

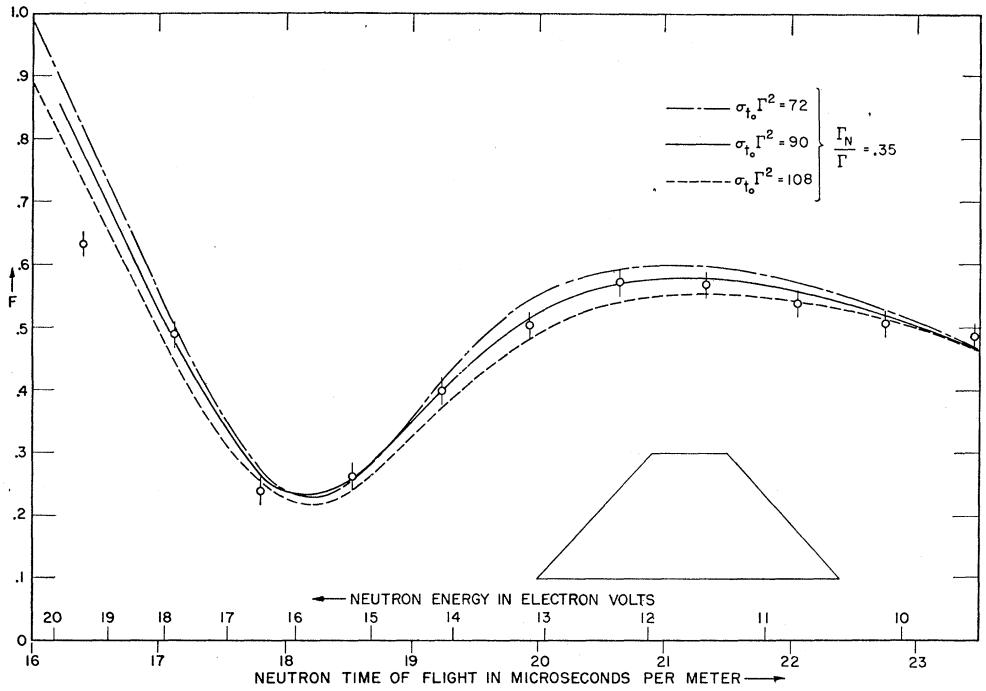

(a)

appeared to be in agreement with other measurements of $\sigma_{t0}\sim 25\,000$ b, (mainly from self-indication experiments). Since then more refined transmission measurements have placed σ_{t0} for gold at 31 000 b,[27,29] and more recently at 37 000 b.[43] A similar situation exists with regard to the silver 5.19-ev level. Early measurements by Coster *et al.*[44] as corrected by Groendijk[11] yielded $\sigma_{t0}=8800$ b for this resonance in the element. Selove[20] obtained 12 000 b, Seidl *et al.*[29] 14 000 b, Draper and Baker[45] 16 000 b, and Wood[37] 16 500 b. This upward trend in the values reported for this parameter has paralleled the concomitant improvement in resolution with which the measurements were made. Consideration of the existing discrepancy in σ_{t0} should therefore take cognizance of the basic difference between the two types of experiments as regards the importance of resolution as well as Doppler effect. The thick-target scattering experiment measures σ_s/σ_t which is a slowly varying function of energy near resonance, and for which the data can be completely resolved. Also the results of Sec. III above indicate that the Doppler effect does not distort the experimental curve measurably. On the other hand, experiments which measure σ_t alone (or σ_s alone) are faced with the difficulty of determining a sharply peaked function that may vary over several orders of magnitude in an extremely narrow energy range near resonance. Evaluation of peak cross sections would therefore require accurate resolution and Doppler corrections. In fact, the only case where agreement has been reached between the results of thick-target scattering and transmission experiments is the scattering measurement by Brockhouse[30] of the 0.176-ev cadmium resonance. In this case the scattering measurement indicated that the accepted value of σ_{t0} for this resonance was too low, and provided the incentive for a careful measurement of the resonance by transmission which raised the value to substantial agreement with the scattering experiment. The energy of this resonance is so low, however, that resolution and Doppler corrections are virtually negligible.

The high resolution of the most recent transmission measurements have reduced the discrepancy in σ_{t0} to $\sim$10 percent for the gold 4.91-ev resonance and $\sim$27 percent for the silver 5.19-ev resonance. In the latter case this represents a sufficiently wide difference that it is doubtful whether further improvement in resolution would close the gap. In fact, the Doppler correction is now considerably greater than the resolution correction in the latest total cross section measurements at $\sim$5 ev. Since the Doppler correction would be greater for silver than for gold, it is possible that a refinement in this correction would serve to reduce the existing discrepancies to the range of experimental error. However, the theoretical basis for such a refinement is not clear at the present time.

In the case of the potential scattering, which does not involve the resonant parameters, the results of the present measurement in silver are in good agreement with values reported by other investigators. Hibdon

[43] Wood, Landon, and Sailor (to be published).
[44] Coster, DeVries, and Diemer, Physica **10**, 281 (1943).
[45] J. E. Draper and C. P. Baker, Phys. Rev. **95**, 644(A) (1954).

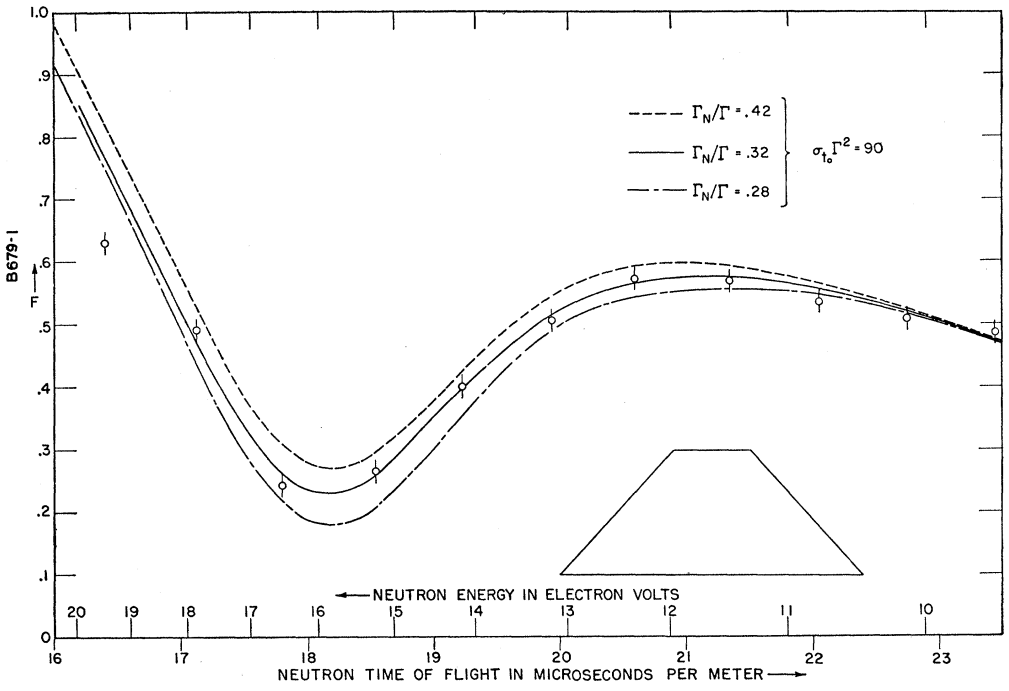

(b)

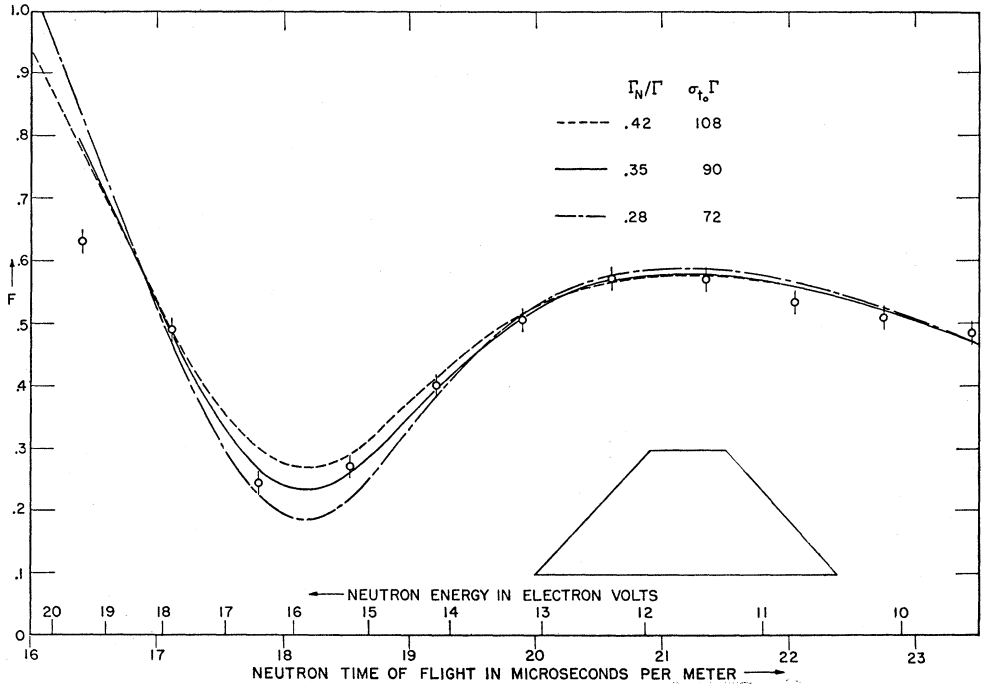

(c)

FIG. 12 Scattering curves for the 16.6-ev level of silver in which the quantities Γ_n/Γ and $\sigma_{t0}\Gamma^2$ are varied by ± 20 percent and the results compared with the "best fit" curve of Fig. 11. (The resolution function shown has been applied to all calculated curves.) Curve A shows a ± 20 percent variation in $\sigma_{t0}\Gamma^2$ with Γ_n/Γ held constant. Curve B shows a ± 20 percent variation in Γ_n/Γ with $\sigma_{t0}\Gamma^2$ constant. Curve C shows a simultaneous ± 20 percent variation in both Γ_n/Γ and $\sigma_{t0}\Gamma^2$.

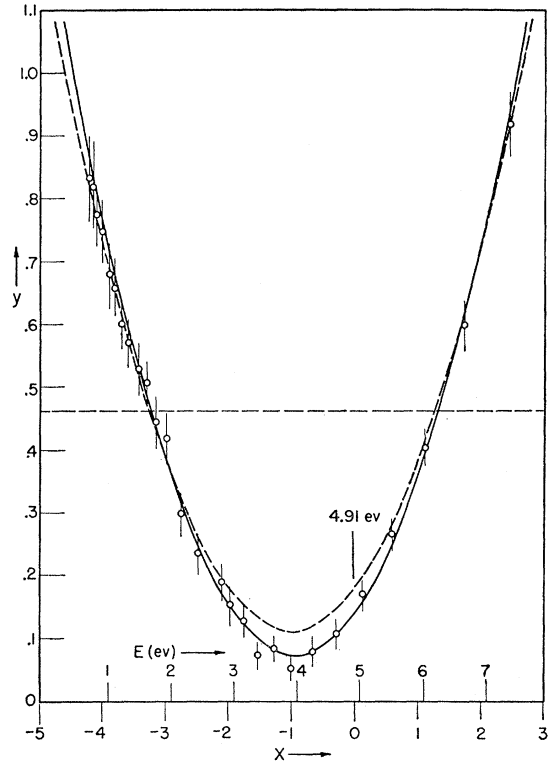

FIG. 13. Parabolic curves analogous to Fig. 7 for the gold 4.91-ev level.

and Muehlhause[39] obtained the values σ_p(element) $=6.50$ b, $\sigma_p(107)=7.91$ b, and $\sigma_p(109)=4.64$ b. More recently, Wood[37] obtained σ_p(element)$=6.0$ b, $\sigma_p(107)$ $=7.3$ b, and $\sigma_p(109)=4.7$ b. These results compare favorably with those listed in Table I.

The results of the present scattering measurements on the 16.6-ev level of silver seem to indicate that the percentage of resonant scattering and the level strength are considerably higher than that obtained from transmission measurements.[3,22,29] The value $\Gamma_n/\Gamma=0.35$ as determined herein, may be subject to doubt since the scattering data for this level were not completely resolved. The disagreement in $\sigma_{t0}\Gamma^2$ however, by a ratio of 3 to 1 constitutes a serious discrepancy because this quantity is insensitive to resolution and Doppler effects when determined by transmission. Therefore improvements in experimental technique would not be expected to raise its value significantly. On the other hand the results shown in Fig. 10 indicate that it would be very unlikely to correlate the scattering results with a value of $\sigma_{t0}\Gamma^2$ below about 60 b-ev^2, especially in the region where there are no appreciable corrections to the data, (18 to 23 μsec/m). This would still leave a discrepancy $\sim$2 to 1. No conclusions can therefore be drawn for this resonance from the present work, except to say that the preliminary results indicate more scattering and a stronger level than reported by other investigators, and that the probable value of J for the level is 0. It is conceivable that higher levels have affected the scattering data more than anticipated. In this respect a thick-target scattering experiment using a target of isotopic Ag^{107} would be highly desirable. This would remove both neighboring levels in the case of the 16.6-ev resonance. Because of material requirements such an experiment would be feasible only with an intense neutron beam of small cross section.

An interesting possibility arises in connection with the apparent distortion from a true Breit-Wigner shape noted in the case of the Ag 5.19-ev level (see Fig. 8). As previously mentioned in the text, this was originally assumed to be due to other levels including a possible negative level near zero energy. As a check on this idea the same type of analysis was performed on the scattering data for the gold 4.91-ev level, the results of which are shown in Fig. 13. The deviation from a parabolic shape is even more pronounced in this case than for the silver. Since this is an isolated level it would be difficult to ascribe the distortion to other levels. The possibility exists that this effect arises from the neglect of second-order terms in the Breit-Wigner formula.

ACKNOWLEDGMENTS

The authors wish to express their appreciation to Dr. Jay Tittman, who collaborated in the initial phases of this research. They are indebted to Professor J. Rainwater and Professor W. W. Havens, Jr. for their active guidance and invaluable suggestions. The authors would also like to thank Dr. David C. Peaslee and Dr. Edward Melkonian for their many helpful suggestions and criticisms, Arthur Layzer for his assistance in working out correction factors, and Miss Miriam Levin for her assistance in the experimental phase of this research. The authors are appreciative of the interesting discussions of these results with R. E. Wood, and Dr. V. Sailor, Dr. H. Foote, and Dr. H. H. Landon, of the Brookhaven Laboratories who also provided comparative data in advance of publication.

Thanks are also due to the U. S. Atomic Energy Commission, which aided materially in the performance of this research.